JOURNAL OF CATALYSIS 76, 84–92 (1982)

Enhancement of Oxygen Transmission in the Oxidation of Active Carbon by the Composite Catalyst

TOMOYUKI INUI, TOSHIRO OTOWA, AND YOSHINOBU TAKEGAMI

Department of Hydrocarbon Chemistry, Faculty of Engineering, Kyoto University, Yoshida, Sakyo-ku, Kyoto 606, Japan

Received October 19, 1981; revised February 18, 1982

Low-temperature oxidation of active carbon in the temperature range 200–500°C on a series of composite catalysts was studied. The oxidation state of the catalyst metal during the reaction was determined at various temperatures by a dynamic adsorption method. The three-component catalyst, Co as the main component of the catalyst combined with small amounts of La_2O_3 and Pt, exerted a synergistic effect on the oxidation activity. The oxidation activities were more enhanced at more reduced states of the catalyst during the reaction. When Pt particles were dispersed close to but separate from Co + La_2O_3 particles, the three-component catalyst accelerated the oxygen uptake and also the oxygen transfer to the carbon. A two-step oxygen transmission mechanism, interpreting the acceleration of oxygen transmission to the active carbon through the Pt and then Co + La_2O_3, is proposed.

INTRODUCTION

Limited global supply of petroleum has recently stimulated extensive study of the production of synthesis gas and SNG by gasification of coal. The use of catalysts in gasification systems is favorable for lowering operation temperature and improving selectivity (*1*). Catalyzed oxidation of carbon is significant for offering the basic knowledge to understand and develop catalysts for other useful reactions such as the water gas reaction ($C + H_2O \rightarrow H_2 + CO$) and the Boudouard reaction ($C + CO_2 \rightarrow 2CO$). Thus, catalyzed oxidation of carbon by molecular oxygen has been widely studied (*2, 3*), using various kinds of catalysts such as metal, metal oxides, and metal salts. In these studies, the relative ranking of catalytic activity and the rate of oxidation were determined by measuring weight decrease with increase of reaction period and obtaining the ignition temperature (*4*). With the progress of microscopic techniques, the topographical and dynamic effects of catalytically active particles during gasification reactions could be directly observed (*5*). However, the samples of carbon species used in previous studies were limited in graphite although their sources were different, and in most cases single-catalyst components were adopted and operation temperatures were considerably high. Furthermore, the oxidation states of the catalyst during the reaction were not extensively studied.

We have previously reported that iron-group metal-based composite catalysts, such as Ni–La_2O_3–Ru, exerted synergistic effects in the direct hydrogenation of carbon (*6*), and these effects were interpreted according to the hydrogen spillover mechanism. Surprisingly, those composite catalysts also exerted synergistic effects in oxidation reactions of carbon by O_2 (*7*) and NO (*8, 9*). However, the mechanism of such enhancing phenomena in oxidation has not been discussed widely. We noted also that a difference in the supporting sequence of the catalyst components gave a large difference in the catalytic activity (*6*). In this paper, therefore, for the two kinds of three-component catalysts, which had the same composition but were prepared in different supporting sequences, the oxidation rate of carbon and the oxidation state of catalyst

0021-9517/82/070084-09$02.00/0

metal during the reaction were measured simultaneously. On the basis of these data, the mechanism of the synergistic effect of the composite catalyst in carbon oxidation was discussed.

EXPERIMENTAL METHODS

Catalysts

The catalyst supported on active carbon was prepared by impregnation of active carbon with catalyst-metal salts. A-3 active carbon, 30–60 mesh in size, prepared by Shimadzu Seisakusho Company Ltd., Japan, was used as the reaction material and, concurrently, as the catalyst support. It had a BET surface area of 1230 $m^2\ g^{-1}$, a porosity of 0.46, a bulk density of 0.38 g cm^{-3}, a macropore of 3 μm in diameter, and a micropore of 26 Å in diameter. The volumetric ratio of the macropore to the micropore was 0.53. A water-soluble component was not detected. Volatile matter was negligible below 500°C in the stream of nitrogen containing 10% hydrogen.

The active carbon was immersed in an impregnating aqueous solution of nitrate salt or chloride of catalyst metal. After thorough drying over a boiling water bath, it was exposed to a saturated vapor of 10% aqueous ammonia solution at 20°C for 2 min, followed by heating in a nitrogen stream containing 10% hydrogen (*6*).

Several weight percent of Co was supported as the main component of the catalyst. La_2O_3 and Pt were added as co-catalysts. The atomic ratios of La and Pt were set at ca. 0.2 and 0.04 of Co, respectively. This mixed solution was used for the preparation of two-component catalysts.

In the case of a three-component catalyst, two preparation methods were used. Method I: nitrate or chloride of each component was impregnated simultaneously on the active carbon (simultaneous supporting method). Method II: the platinum was first dispersed, and the other two components were then supported (two-step supporting method).

Changes of shape of the active carbon and of the catalyst, accompanying the progress of the reaction, were observed using a scanning electron microscope (Hitachi-Akashi MSM 4C-102, resolution 70 Å).

Reaction Operation

An ordinary flow reaction apparatus was used at atmospheric pressure. A quartz tube with an inner diameter of 4 mm was chosen as the reactor. A 10-mg (0.026-cm^3) portion of the catalyst was packed in the reactor, which was heated by an external electric furnace. The catalyst-bed temperature was measured by inserting the top of a thermocouple shielded with stainless steel of 0.6 mm diameter into the exit side of the catalyst bed.

One percent of oxygen diluted with nitrogen was fed from a cylinder, through a pressure reducer, needle valve, and flowmeter. The flow rate of feed gas was set at 50 cm^3 STP min^{-1} so that the initial space velocity was $11.5 \times 10^4\ h^{-1}$.

Dynamic Adsorption Measurement

The dynamic adsorption method using a TCD-type gas chromatograph (*10*) was applied in order to determine the oxidation state of the catalyst metal during the reaction.

Oxygen was introduced in a step-function manner to a sample cell packed with a reduced catalyst metal. From the analysis of the breakthrough curve and elution curve, an apparent O_2 uptake was obtained. A portion of the effluent gas was analyzed frequently by another gas chromatograph during the course of the step-function response, and carbon oxides formed were analyzed. The apparent O_2 uptake was corrected by the amount of carbon oxides formed, and the oxidation state of the catalyst metal during the carbon oxidation reaction was calculated. The apparatus and procedure were as follows:

A glass tube with an inner diameter of 5.0 mm was used as the catalyst-sample cell. The passage between the sample cell and

the thermal conductivity detector was connected with a glass capillary of 2 mm i.d. to minimize the dead space. The dead space was only 5 cm^3, and a quick gas chromatographic response was achieved.

A 100-mg (0.26-cm^3) portion of the catalyst sample was packed into the sample cell. The bed length was 1.5 cm. The temperature of the sample cell was controlled to within ±0.3°C by an outside electric furnace. The temperature of the sample was measured by a thermocouple in contact with the exit of the bed.

Before the measurement, the sample was treated *in situ* by 5% of H_2 diluted by helium with a flow rate of 30 cm^3 min^{-1} at 400°C for 10 min. Then it was set for a certain temperature under the flow of the carrier gas (He). The carrier gas was purified by passing through a heated column packed with a 5.0% Cu/Al_2O_3 catalyst and a silica gel column, to remove oxygen and water, respectively.

The adsorption gas containing a certain concentration of O_2 diluted with helium was introduced at the same flow rate as the carrier gas. This procedure was effected immediately by operating a four-way valve located just at the entrance of the sample cell. All gas flows were controlled by precision flow-rate controllers.

After confirming the breakthrough and subsequent attainment of a constant level for the detector response, the supply of adsorption gas was substituted by the carrier gas. From this time, the elution curve was recorded. The same operation was carried out for the support, to correct for the apparatus's dead space, the pore volume of the catalyst support, and the amount of oxygen adsorbed on the support. A portion of effluent gas was analyzed by gas chromatograph with columns of Porapak Q for CO_2 and MS-5A for O_2 and CO, respectively.

RESULTS AND DISCUSSION

Synergistic Effect of the Catalyst Component

In previous studies on the reactivities of catalysts in carbon oxidation, ignition temperature was usually examined as a criterion for catalytic activity (*4*). The ignition temperature, however, cannot assure the magnitude of steady-state rate of the carbon combustion and/or the degree of carbon consumption. This is due to the fact that, accompanying the carbon consumption, the oxidation state of the catalyst metal and the state of contact between catalyst particles and carbon may change, and therefore, the catalytic activity may largely decrease.

On the other hand, CO_2 yield per unit reaction period (Y_{CO_2}) or the integral of Y_{CO_2} for a certain period of the first reaction stage reflects the real catalytic activity more practically. From this viewpoint, the changes of Y_{CO_2} with reaction period at 500°C for various catalysts were compared in Fig. 1. An upper constant level of the curve corresponds to the complete conversion of oxygen fed. The three-component catalyst kept this level for the longest reaction period. It also completely consumed carbon within the fastest reaction period among four kinds of catalysts, i.e., the three-component catalyst exerted the highest activity.

The integral amount of Y_{CO_2} for the first 50 min was compared for each catalyst at which the carbon support of the three-component catalyst was almost completely con-

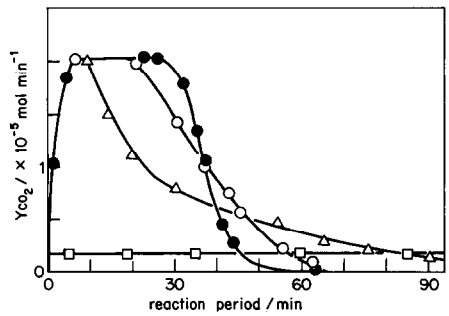

FIG. 1. Change of carbon dioxide yield with reaction period for various Co-based composite catalysts. Reaction temperature: 500°C; feed gas composition: 1.0% O_2; flow rate: 46 cm^3 min^{-1}; weight of catalyst used: 10 mg; □: 0.7% Pt/C; △: 4.7% Co/C; ○: 4.6% Co + 2.7% La_2O_3/C; ●: 4.6% Co + 2.7% La_2O_3 + 0.7% Pt/C.

verted. The values for the four catalysts of Co + La_2O_3 + Pt/C, Co + La_2O_3/C, Co/C, and Pt/C were 7.48, 7.10, 5.38, and 1.06 × 10^{-4} mol, respectively.

The decrease of Y_{CO_2} with reaction period owing to carbon consumption was different in each catalyst. In Co + La_2O_3/C and Co + La_2O_3 + Pt/C catalysts, the carbon was completely consumed by the 65-min point, whereas the amounts of carbon burn-off in Co/C and Pt/C at 65 min were 74 and 12%, respectively. Further, it was found that the oxidation activity of the three-component catalyst was considerably affected by the supporting sequence of the catalyst components on the active carbon, i.e., as will be shown later in Fig. 6, the activity of the catalyst system of method II was greater than that of method I. Such an effect has been observed on both methanation of carbon oxides (*11*) and direct hydrogenation of carbon (*6*) over similar composite catalysts.

Characteristics of Oxygen Adsorption

In order to clarify the oxygen mobility through the catalyst to the active carbon, the dynamic adsorption measurement was introduced in this study. In almost all cases, when oxygen was introduced into the adsorption-gas flow, it was taken up completely on the catalyst for a while, then the breakthrough occurred suddenly. This indicates that a rapid and strong adsorption was predominant. A very small amount of oxygen was desorbed in the course of elution so that the oxygen was regarded as apparently being adsorbed irreversibly, i.e., the catalyst metal was oxidized. As shown in Fig. 2, a single breakthrough curve for oxygen was obtained below 200°C, where oxidation of carbon was negligible. However, above 200°C the breakthrough curve showed a stepwise shape, as in Fig. 3. On the basis of the analysis of effluent gas, the first step of the breakthrough curve corresponded to the eluted CO_2, and the second step of the curve appearing after 13 min was eluted oxygen. The amount of CO in this temperature region was negligible. At temperatures over 400°C, oxygen conversion reached 100%, and a single breakthrough curve for CO_2 containing small amounts of CO was obtained. A similar curve was also obtained for CO_2 containing unreacted O_2 when the oxygen concentration was in excess for the complete conversion. The breakthrough curve of the support carbon was shown as a broken line in Figs. 2 and 3, which was close to the response of dead space, and the amount of adsorbed oxygen on the carbon support was very small in the entire range of temperatures. Therefore, in these figures the hatched area corresponds to the amount of adsorbed oxygen (T_a) on the catalyst metal under the given oxygen concentration.

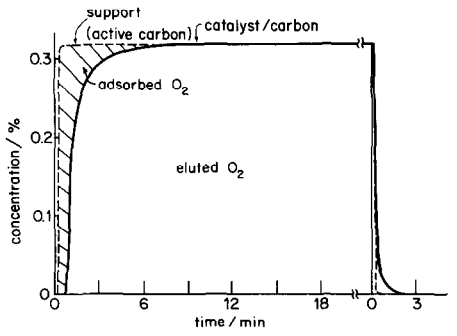

FIG. 2. Adsorption and desorption diagram for O_2 on a catalyst at 200°C. Sample: the three-component catalyst prepared by method II; solid line: catalyst/carbon; broken line: carbon support.

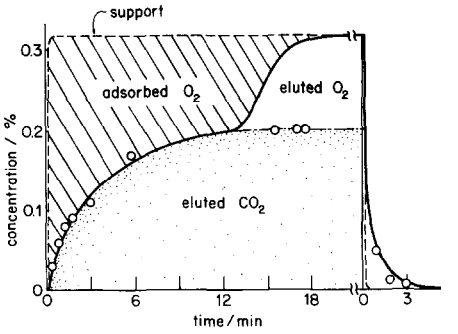

FIG. 3. Diagram of simultaneous measurements of O_2 adsorption and CO_2 formation at 300°C. Sample: the three-component catalyst prepared by method I; solid line: catalyst/carbon; broken line: carbon support; O: CO_2 content analyzed by another gas chromatograph.

The amount of the irreversible oxygen adsorption (I_a) was obtained from the difference between T_a and the eluted oxygen (T_d). Isobars of I_a for both Co + La_2O_3 + Pt/C catalysts prepared by methods I and II are shown in Figs. 4 and 5.

In order to estimate the oxidation state of the main catalyst component, i.e., Co in Co + La_2O_3 + Pt/C catalyst, we assumed for convenience that I_a was used for oxidizing only Co metal. The rate of oxygen adsorption on Pt was certainly rapid; however, since the capability of the Pt component is ca. 1/35th of that of the Co component assuming the ultimate oxide forms are PtO and Co_2O_3, respectively, the amount of oxygen adsorbed on Pt was considered to be negligible. The oxidation state of Co was approximately estimated as the y value in CoO_y.

The common feature of the temperature dependence of I_a in Figs. 4 and 5 was that I_a increased with elevating temperature and after attaining a maximum level I_a decreased, irrespective of oxygen concentration and kind of catalyst. In a higher-temperature range, over 350–400°C, I_a's of both catalysts were apt to approach the zero level, i.e., the reduced metallic state.

Evident differences of temperature dependence of I_a between the two kinds of catalysts were as follows: Compared with

FIG. 4. Temperature dependence of the irreversible O_2 adsorption on the catalyst prepared by the two-step supporting method (method II). Catalyst used: 4.6% Co + 2.7% La_2O_3 + 0.7% Pt/C, 100 mg; O_2 concentrations: △, 0.3%; □, 0.5%; ◑, 1.0%; ○, 3.0%; flow rate: 30 cm^3 min^{-1}.

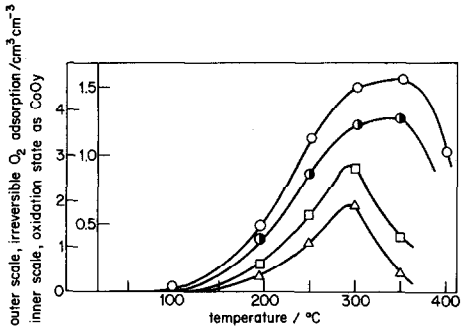

FIG. 5. Temperature dependence of the irreversible O_2 adsorption on the catalyst prepared by the simultaneous supporting method (method I). Catalyst used: 5.0% Co + 2.8% La_2O_3 + 0.7% Pt/C, 100 mg; O_2 concentrations: △, 0.3%; □, 0.5%; ◑, 1.0%; ○, 3.0%; flow rate: 30 cm^3 min^{-1}.

the method I catalyst, the I_a of the method II catalyst increased from a lower temperature and began to decrease at lower temperatures. Furthermore, the values of I_a or y of the method II catalyst were smaller than those of the method I catalyst. At a high O_2 concentration such as 3.0%, maximum oxidation states of Co for the method II and I catalysts were about CoO and $CoO_{1.5}$ (i.e., Co_2O_3), respectively.

Catalytic Activity of Carbon Oxidation

The carbon-oxidation activities of catalysts of both methods I and II were measured at several temperatures. Converted O_2 (mol) at the steady state measured in the dynamic adsorption measurement at each temperature is plotted in Fig. 6. The upper limit of this figure corresponds to the complete O_2 conversion. The converted O_2 up to ca. 450°C was used completely for the CO_2 formation according to the equation

$$C + O_2 \rightarrow CO_2. \qquad (1)$$

From the comparison at the low-temperature range, it is clear that the carbon-oxidation rate of the catalyst of method II was higher than that of method I, and both rates were far higher than the rate of noncatalyzed oxidation of the carbon support.

At temperatures higher than 450°C, the converted O_2 was used partly for CO forma-

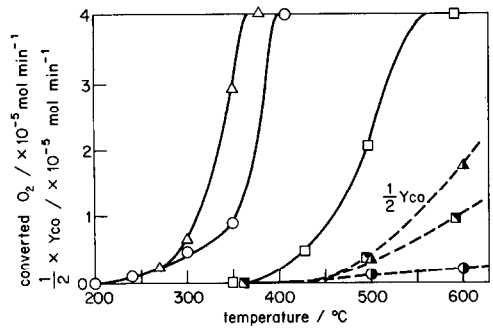

FIG. 6. Comparison of the oxidation rate and Y_{CO} of the catalysts of methods I and II. Catalyst used: the three-component catalyst, 100 mg; feed gas composition: 3.0% O_2 and 97% He; flow rate: 30 cm^3 min^{-1}; ○,◑: method I; △,◭: method II; □,◩: the carbon support; solid line: converted O_2; broken line: $\frac{1}{2}$ × rate of CO formation ($\frac{1}{2}Y_{CO}$).

tion, and the order of CO yield (Y_{CO}) was, the catalyst of method II > the carbon support > the catalyst of method I, which differs from the order of CO_2 formation at the lower-temperature range. In the case of the carbon support, CO_2–CO composition in the effluent gas was close to equilibrium (*12*). This indicates that the incomplete combustion reaction (Eq. (2)) proceeded simultaneously with the complete combustion reaction (Eq. (1)), and Eqs. (3) and (4) attained equilibrium.

$$C + \tfrac{1}{2}O_2 \rightarrow CO, \qquad (2)$$

$$C + CO_2 \rightarrow 2CO, \qquad (3)$$

$$2CO \rightarrow C + CO_2. \qquad (4)$$

In the cases of the catalysts of methods I and II, the oxidation rate was so rapid that when CO formed according to Eq. (2), the CO converted immediately to CO_2 by successive oxidation (Eq. (5)) as shown in the case of the catalyst of method I.

$$CO + \tfrac{1}{2}O_2 \rightarrow CO_2. \qquad (5)$$

Therefore, the cause of the increase of CO beyond CO–CO_2 equilibrium in the case of the catalyst of method II was naturally considered to be that the Boudouard reaction (Eq. (3)) proceeded catalytically.

In order to clarify the difference of CO formation in the high-temperature range, both catalysts were treated under the same flow condition with the reaction gas, in which CO_2 substituted for O_2 (i.e., 3.0% CO_2 + 97% He). The Y_{CO} in this experiment agreed with the Y_{CO} in Fig. 6 for each catalyst, and the above-mentioned cause was confirmed. The correspondence of the catalytic reactivities between the reactions of Eqs. (1) and (3) is noteworthy. Details of this result will be discussed elsewhere (*13*).

Correspondence of the Oxidation Activity to the Oxidation State of the Catalyst Metal

Change in CO_2 concentration with reaction period was independently analyzed by gas chromatography in the dynamic adsorption measurement, and was shown in Figs. 7 and 8. For the catalyst of method I, CO_2 formation at 300°C (Fig. 7) increased in the early stage and began to decrease with the progress of the reaction period, except for the lowest O_2 concentration (0.45%). After about 10 min, CO_2 formation coincided irrespective of O_2 concentration. These features were the same at 350°C (Fig. 8), whereas the CO_2 formation for each O_2 concentration increased to twice as much as that at 300°C.

For the catalyst of method II, CO_2 forma-

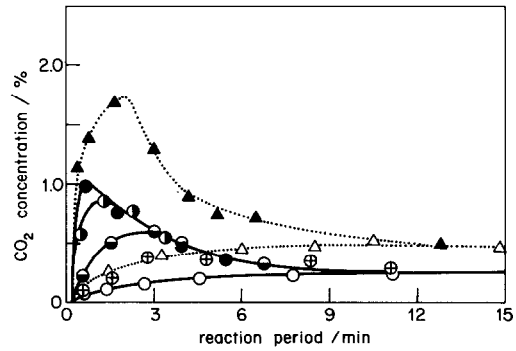

FIG. 7. Change in CO_2 concentration in the effluent gas with reaction period at 300°C. Catalyst used: Co + La_2O_3 + Pt/C, 100 mg; flow rate: 30 cm^{3}min^{-1}; O_2 concentrations: ●, 4.9%; ◑, 3.6%; ▲, 3.2%; ◒, 2.1%; ⊕, 1.0%; △, 0.75%; ○, 0.45%; solid line: the catalyst of method I; dotted line: the catalyst of method II.

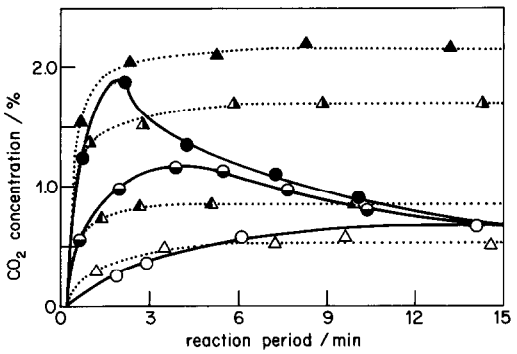

FIG. 8. Change in CO_2 concentration in the effluent gas with reaction period at 350°C. Catalyst used: Co + La_2O_3 + Pt/C, 100 mg; flow rate: 30 cm^3 min^{-1}; O_2 concentrations: ●, 3.4%; ▲, 3.0%; ◭, 2.1%; ◒, 2.0%; ◮, 1.1%; ○, 0.79%; △, 0.61%; solid line: the catalyst of method I; dotted line: the catalyst of method II.

tion at 300°C was greater than that for the catalyst of method I, but still showed the same feature as in the latter case. However, at a higher temperature such as 350°C, as can be seen in Fig. 8, CO_2 formation maintained a steady state for each O_2 concentration. These facts correspond well to the characteristics of the O_2 adsorption shown in Figs. 4 and 5.

Since the hydrogen reduction was conducted prior to the adsorption measurement, the catalyst had been reduced in the early stage, so that the transfer of oxygen on the catalyst metal was rapid, and CO_2 formation was large. As shown in the case of 300°C when the oxidation rate of the catalyst metal exceeded the oxidation rate of carbon, the oxidation state of the catalyst metal proceeded to a higher level with the reaction period resulting in a lower catalytic activity. For the catalyst of method II, at 350°C the CO_2 formation at the steady state increased with the increase of O_2 concentration. Further, at higher O_2 concentrations the oxidation states were somewhat lower than those of the case of the catalyst of method I, namely, a higher catalytic activity was shown on a more reduced state of catalyst.

Since the chemical composition and dispersion degree of the main component part (Co + La_2O_3) of both catalysts were the same, there must be no difference in the maximum capacity of oxygen uptake and in capability for the reduction of the oxidized catalyst metal by carbon. Therefore, the considerable difference in the activity of carbon oxidation, and in the oxygen uptake during the reaction for both catalysts, is attributed to the difference in the rate of oxygen transfer from the ambient phase to the carbon phase via the surface of catalyst particles. At the steady state of the carbon oxidation, this mechanism (*14*) may coincide microscopically with the redox mechanism (*2*) which has been considered as a sequential combination of the reactions referred to as Eqs. (6) and (7).

$$MO_y + O \rightarrow MO_{y+1}, \quad (6)$$

$$2MO_{y+1} + C \rightarrow CO_2 + 2MO_y. \quad (7)$$

However, under a non-steady-state condition, we can see the two separate reactions as follows: With the catalyst of method II, after confirming the steady state of the carbon oxidation with 0.3% O_2 gas flow at 250°C, the catalyst temperature was elevated to 350°C at a constant rate of 10°C/min in an inert gas (N_2) flow. The oxidation state of the Co metal at 250°C ($CoO_{0.45}$) changed to $CoO_{0.40}$ at 350°C and differed from the value ($CoO_{0.14}$) in the case being treated directly at 350°C. This fact indicated that the rate of reaction between carbon and the partly oxidized Co (i.e., Eq. (7)) was affected by the oxidation state of Co itself, and the oxidation state during the steady-state reaction at each temperature was determined by the dynamic balance of the reactions of Eqs. (6) and (7).

Effect of Oxygen Concentration on the Oxidation Activity

Dependence of O_2 concentration on Y_{CO_2} at the steady state for both catalysts is shown in Fig. 9. All the Y_{CO_2} except one case (the catalyst of method II, 350°C), gave respectively constant values in the region of incomplete O_2 conversion, indicat-

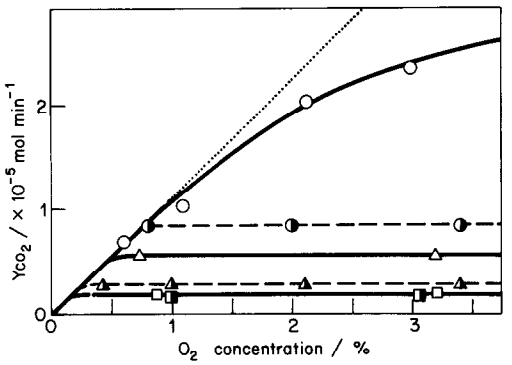

FIG. 9. Effect of oxygen concentration on the yield of carbon dioxide for the catalysts of methods I and II. □, ◨: 270°C; △, ◭: 300°C; ○, ◑: 350°C; half-filled symbols; the catalyst of method I; open symbols: the catalyst of method II; dotted line corresponds to the total conversion of oxygen.

ing that the rate-determining step was the process of oxygen transfer on the catalyst phase. However, the Y_{CO_2} in the exceptional case increased with the increase of O_2 concentration at least up to 3.0%, indicating that the rate-determining step was the process of oxygen uptake, and that oxygen transfer on the catalyst phase was very rapid.

The oxidation states of the catalysts of methods I and II under the conditions of 3.0% O_2 and 350°C were $CoO_{1.5}$ and $CoO_{0.50}$, respectively, as shown in Figs. 4 and 5. Thus, it was reconfirmed that the oxidation activity was more enhanced at the more reduced state of the catalyst metal during the reaction, and this agreed with the fact observed by Walker *et al.* (*2*).

Pitting Mechanism

Photographs taken with the scanning electron microscope in Fig. 10 show the catalyst before the reaction and after 30 min of reaction period. Many pore openings have been generated. This indicates that the reaction proceeds from the surface in contact with the catalyst crystallite into the bulk of the active carbon as though a hole is being dug by the catalyst crystallite. Such a contact mechanism/pitting mechanism is commonly accepted in the catalytic oxidation of graphite, which was studied applying an *in situ* electron microscopy technique (*5*).

Two-Step Oxygen Transmission Mechanism

In comparison with the catalyst of

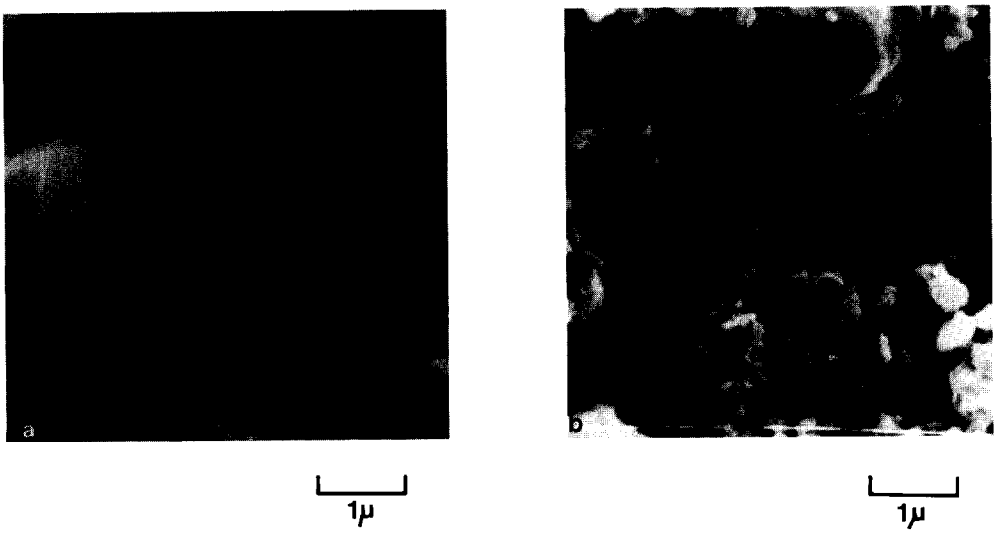

FIG. 10. SEM photographs of the catalyst supported on active carbon before and after the reaction. Catalyst: 4.6% Co + 2.7% La_2O_3 + 0.7% Pt/C (method II); (a) before the reaction; (b) after the reaction (500°C, carbon conversion: 53%).

method I, the catalyst of method II increases O_2 uptake from a lower temperature and accelerates to a greater extent the oxygen transfer during the oxidation of carbon. This fact is interpreted, with regard to the synergistic effect, as the two-step catalytic mechanism (*6*) as follows:

When three components are supported simultaneously as in method I, platinum particles are probably in the mixed phase of Co + La_2O_3 and Pt's own activity is fairly hidden. On the contrary, when platinum is dispersed on the support prior to Co + La_2O_3 as in method II, a number of platinum particles exist separately from Co + L_2O_3 particles. Dispersed particles of Pt have a high rate of oxygen adsorption but are easily reduced; thus the Pt particles, which are located in contact with the particles of Co + La_2O_3, play the role of the porthole of oxygen uptake and transmit oxygen into the Co + La_2O_3 part. The oxygen in the partially oxidized Co + La_2O_3 part then reacts with carbon. The oxygen transfer is regarded as one of the driving forces accounting for the random mobility of catalyst particles widely observed (*5*) in carbon oxidation.

In conclusion, the first transmission of oxygen occurs from Pt to Co + La_2O_3, then the second one occurs from Co + La_2O_3 particles, which are the main component of the catalyst, to the carbon phase. Since such a phase separation in the catalyst component accelerated the oxygen transfer, it synergistically enhanced the oxidation reaction. This mechanism may be called a two-step oxygen transmission mechanism, which is a concept similar to that of the hydrogen spillover on the composite catalyst supported on active carbon (*6, 10*).

REFERENCES

1. Johnson, J. L., *Catal. Rev.* **14,** 131 (1976).
2. Walker, P. L., Jr., Shelef, M., and Anderson, R. A., *in* "Chemistry and Physics of Carbon," Vol. 4, p. 287. Dekker, New York, 1968.
3. McKee, D. W., *in* "Chemistry and Physics of Carbon," Vol. 16, p. 1. Dekker, New York, 1980.
4. McKee, D. W., *Carbon* **8,** 131, 623 (1970).
5. Baker, R. T. K., and Sherwood, R. D., *J. Catal.* **61,** 378 (1980).
6. Inui, T., Ueno, K., Funabiki, M., Suehiro, M., Sezume, T., and Takegami, Y., *J. Chem. Soc. Faraday Trans. 1* **75,** 1495 (1979).
7. Inui, T., Otowa, T., Tstuchihashi, K., and Takegami, Y., *Carbon, 20,* (1982).
8. Inui, T., Otowa, T., and Takegami, Y., *J. Chem. Soc. Chem. Commun.,* 94 (1980).
9. Inui, T., Otowa, T., and Takegami, Y., *Ind. Eng. Chem. Prod. Res. Dev.* **21,** 56(1982).
10. Inui, T., Funabiki, M., and Takegami, Y., *J. Chem. Soc. Faraday Trans. 1* **76,** 2237 (1980).
11. Inui, T., Funabiki, M., Suehiro, M., and Sezume, T., *J. Chem. Soc. Faraday Trans. 1* **75,** 787 (1979).
12. Walker, P. L., Jr., Rusinko, F., Jr., and Austin, L. G., *in* "Advances in Catalysis and Related Subjects," Vol. 11, p. 133. Academic Press, New York/London, 1959.
13. Inui, T., Otowa, T., and Takegami, Y., to be submitted.
14. L'Home, G. A., Boudart, M., and D'Or, L., *Bull. Cl. Sci. Acad. R. Belg.* **52,** 1206, 1249 (1966).